Performance Improvement of 16 QAM Signal in PCN Channel

Eon Gon Kim, Chang Heon Oh, and Sung Joon Cho

Abstract

In this paper, we have analyzed the error performance of the optimum threshold detection (OTD) of 16 QAM signal in the Rician fading channel with and without the maximal ratio combining (MRC) diversity technique in the presence of cochannel Rayleigh interference. And also the error performance of OTD is compared to that of conventional threshold detection (CTD) in the Rician fading channel in the presence of cochannel Rayleigh interference.

With the result of analysis, it is found that there exists a synergistic effect due to both MRC diversity and optimum threshold detection in the Rician fading channel in the presence of cochannel Rayleigh interference.

I. Introduction

Recently, there is a great demend of mobile service and personal communication services. To keep up with the demand, the development and standardization in these services are progressed in several countries [1], [2].

In the personal communication systems which require a high channel capacity and limited bandwidth usage, frequency reuse is essential in increasing spectrum efficiency and a multi-level modulation method is desirable. The presence of cochannel interference because of frequency reuse is seen to be a major problem in personal communication systems. There is a assumption that an undesired signal from a distant cochannel cell may well be modeled by Rayleigh statistics but Rician fading may be a good model for the desired signal since a line-of-sight path may exist within a microcell [3]. The key point in microcell interference modeling is that the desired and undesired signals should have different statistical characteristics. One such interference model is introduced in Ref. [4] The desired signal is assumed to have Rician statistics implying that a dominant multipath exists in within-cell transmission. The interference signals from cochannel cells are assumed to be subject to Rayleigh fading because of the absence of a line-of-sight propagation [4].

In terms of the power and frequency efficiency, 16 QAM is a very attractive multi-level modulation technique [5].

However, 16 QAM has a poor error performance in a fading channel due to its inherent nature of having different levels for different symbols. Therefore, to improve the error performance, adaptive threshold detection technique which is controlled by the ratio of the direct-to-diffuse received signal power is proposed in the Rician fading channel [6].

This paper is devoted to the theoretical performance analysis of the optimum threshold detection (OTD) of 16 QAM signal in the Rician fading channel with and without maximal ratio combining (MRC) diversity technique in the presence of cochannel Rayleigh interference.

II. Analysis Model

Fig. 1 illustrates the schematic diagram of the analysis model. Passing through the Rician fading channel, the desired 16 QAM signal is corrupted by multipath fading resultant from receiving of a direct component and random diffuse component.

This fading imposes random amplitude and phase onto the modulated 16 QAM signal. Besides, the transmitted signals are also corrupted by additive white Gaussian noise (AWGN) and interference signal from cochannel cell which is subjected to Rayleigh fading. The received signals in each diversity branch are weighted proportionately to their carrier to noise power ratios and summed by MRC diversity circuit.

The output signal from the MRC diversity process is

Manuscript received November 15, 1995; accepted November 25, 1995.
E.G.Kim is with Department of Inform. & Comm. Eng., Taejon National Univ. of Technology, Taejon, Korea

C.H.Oh is with Communication System R&D Center, Samsung Electronics Co., Ltd.

S.J.Cho is with Department of Telecomm. and Infor. Eng., Hankuk Aviation University, Kyunggi-Do, Korea.

delivered to the 16 QAM demodulator. In the 16 QAM demodulator, we adopted adaptive threshold detection which is controlled by the direct-to-diffuse signal ratio.

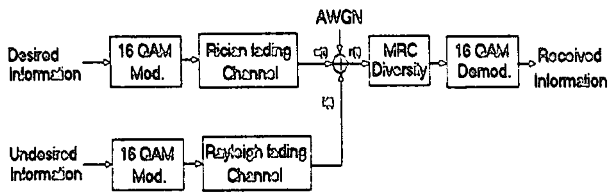

Fig. 1. Analysis model.

The modulated 16 QAM signal can be expressed as [7]

$$s_{16QAM}(t) = a_i(t)\ \cos\omega_c t + b_i(t)\ \sin\omega_c t \qquad (1)$$

where ω_c is the angular carrier frequency, $a_i(t)$ and $b_i(t)$ are the ith in-phase (I) and quadrature (Q) components of the modulated 16 QAM signal.

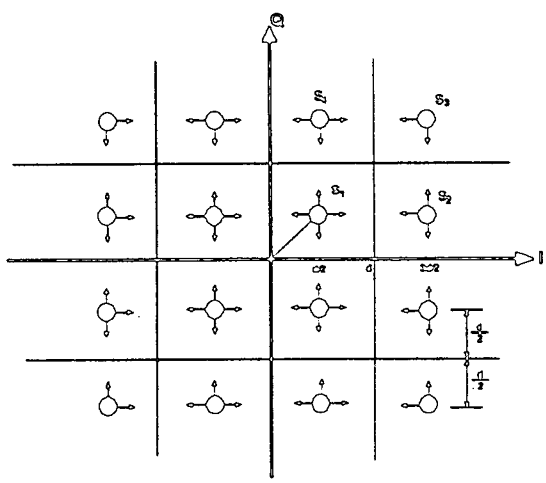

Fig. 2. 16 QAM constellation.

Fig. 2 illustrates a 16 QAM constellation where each dot represents the position of the phasor relative to the intersection of axes marked I (for in-phase) and Q (for quadrature). In Fig. 2, the arrows from dots represent the error directions of the phasors. It also shows that the minimum distance between two signal point is d. In the analysis model shown in Fig. 1, it is assumed that the fading varies very slowly compared to the signaling rate so that the received signal envelope is constant during one signal interval of duration Ts and there is no pass loss between transmitter and receiver. The received signal power can be expressed as

$$\begin{aligned} P_{RX} &= P_{direct} + P_{diffuse} \\ &= A^2 P_{TX} + P_{diffuse}, \quad 0 \le A^2 < 1. \end{aligned} \qquad (2)$$

Deriving from Eq (2), A is $\sqrt{K/K+1}$ where K is a direct component to diffuse component ratio ($P_{direct}/P_{diffuse}$). The received 16 QAM signal is divided into I and Q components which are statistically independent. The I component is Gaussian distributed and its mean is the I component of a direct signal envelope. Fig. 3 illustrates the pdf's of the I components of the received 16 QAM signal corrupted by the Rician fading. Notice that Fig. 3 only shows the pdf's for the dots in the first quadrant of Fig.2.

When the I components of the transmitted 16 QAM signal are $d/2$ and $3d/2$, the pdf's of I components of the received 16 QAM signal corrupted by the Rician fading are described as

$$p_1(x) = \frac{1}{\sqrt{2\pi}\,\sigma_1^2} \exp\left\{ -\frac{(x - A\frac{d}{2})^2}{2\sigma_1^2} \right\}, \qquad (3a)$$

$$p_2(x) = \frac{1}{\sqrt{2\pi}\,\sigma_2^2} \exp\left\{ -\frac{(x - A\frac{3d}{2})^2}{2\sigma_2^2} \right\}, \qquad (3b)$$

where σ_1^2 and σ_2^2 are the variances of signal points.

Notice that the variance σ_2^2 is 9 times larger than σ_1^2 since the variances are proportional to signal powers.

And interference signal from a distant cochannel cell can be expressed as

$$\begin{aligned} I(t) &= I\cos(\omega_c t + \phi) \\ &= I\cos\phi\ \cos\omega_c t - I\sin\phi\ \sin\omega_c t \\ &= I_c\cos\omega_c t - I_s\sin\omega_c t \end{aligned} \qquad (4)$$

where ϕ is the phase of $I(t)$, I_c and I_s are I and Q component of $I(t)$.

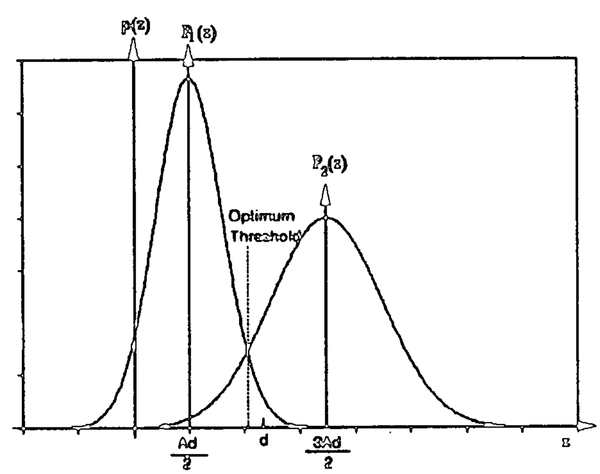

Fig. 3. The pdf's of the I components of the received 16 QAM signal.

Since I is Rayleigh distributed, and ϕ is uniform distributed, I_c and I_s are all Gaussian distributed with zero means and their pdf's are [8]

$$p(I_c) = \frac{1}{\sqrt{2\pi\,\sigma_I^2}} \exp\left\{-\frac{I_c^2}{2\,\sigma_I^2}\right\}, \tag{5a}$$

$$p(I_s) = \frac{1}{\sqrt{2\pi\,\sigma_I^2}} \exp\left\{-\frac{I_s^2}{2\,\sigma_I^2}\right\}, \tag{5b}$$

where σ_I^2 is the variance of $I(t)$.

And I and Q components of the narrowband Gaussian noise $n(t)$ which is randomly added regardless of the transmitted signal are Gaussian distributed with zero means, and the variance of them are σ_n^2.

III. Performance Analysis Without Diversity

1. Conventional Threshold Detection (CTD)

I component of the received 16 QAM signal corrupted by the Rician fading is Gaussian distributed as well as the I component of interference signal and noise. Thus, $p(z) = p(x + I_c + n_c)$, the pdf of the sum of them must be a Gaussian distribution [8]. When the I components of the transmitted signals are $d/2$ and $3d/2$, the pdf's are given as follows;

$$p_1(z) = \frac{1}{\sqrt{2\pi(\sigma_1^2+\sigma_I^2+\sigma_n^2)}} \exp\left\{-\frac{(z - \frac{Ad}{2})^2}{2(\sigma_1^2+\sigma_I^2+\sigma_n^2)}\right\}, \tag{6a}$$

$$p_2(z) = \frac{1}{\sqrt{2\pi(\sigma_2^2+\sigma_I^2+\sigma_n^2)}} \exp\left\{-\frac{(z - \frac{A3d}{2})^2}{2(\sigma_2^2+\sigma_I^2+\sigma_n^2)}\right\}. \tag{6b}$$

The error probabilities of three cases mentioned above are defined as P_{ICA}, P_{ICB}, and P_{ICC}, respectively,

$$P_{ICA} = \int_{-\infty}^{0} p_1(z)\,dz = \frac{1}{2}\,\mathrm{erfc}\left[\sqrt{\frac{K\cdot\gamma_n\cdot\gamma_I}{5(1+K)(\gamma_n+2\gamma_I)+\gamma_n\cdot\gamma_I}}\right], \tag{7a}$$

$$P_{ICB} = \int_{-\infty}^{d} p_2(z)\,dz = \frac{1}{2}\,\mathrm{erfc}\left[\sqrt{\frac{4(K+1)\cdot\gamma_n\cdot\gamma_I}{5(K+1)(\gamma_n+2\gamma_I)+9\gamma_n\cdot\gamma_I}}\cdot\left(\frac{3}{2}\sqrt{\frac{K}{K+1}}-1\right)\right], \tag{7b}$$

$$P_{ICC} = \int_{-\infty}^{d} p_1(z)\,dz = \frac{1}{2}\,\mathrm{erfc}\left[\sqrt{\frac{4(K+1)\cdot\gamma_n\cdot\gamma_I}{5(K+1)(\gamma_n+2\gamma_I)+9\gamma_n\cdot\gamma_I}}\cdot\left(1-\frac{1}{2}\sqrt{\frac{K}{K+1}}\right)\right]. \tag{7c}$$

where γ_I and γ_n is the ratio of the average signal power received to the interference and noise power, respectively.

Letting P_{QCA}, P_{QCB}, and P_{QCC} be the error probabilities of the Q components for the 16 QAM signal for the first quadrant in Fig. 2, their error probabilities are equal to P_{ICA}, P_{ICB}, and P_{ICC}, respectively. Note that the I and Q components are statistically independent each other.

Thus, the total error performance of the 16 QAM signal points labelled S_1, S_2, S_3 and S_4 in Fig. 2 is given below;

$$\begin{aligned} P_1 &= P_{S1} + P_{S2} + P_{S3} + P_{S4} \\ &= 4(P_{ICA} + P_{ICB} + P_{ICC}) - (P_{ICA} + P_{ICB} + P_{ICC})^2 \end{aligned} \tag{8}$$

where P_{S1}, P_{S2}, P_{S3}, and P_{S4} are the error probabilities of 16 QAM signal points of S_1, S_2, S_3 and S_4, respectively.

The average error performance with CTD in Rician fading environment is given below;

$$P_{EC} = \frac{4P_1}{16} = P_{ICA} + P_{ICB} + P_{ICC} - \frac{1}{4}(P_{ICA} + P_{ICB} + P_{ICC})^2, \tag{9}$$

2. Optimum Threshold Detection (OTD)

We suggest that optimum threshold level (OTL) for the Rician fading channel is determined to be the point where $p_1(z) = p_2(z)$ on the I axis as

$$z_{opt} = \frac{3}{8}d\left[\frac{\sqrt{K}+\sqrt{K+\ln 3}}{\sqrt{1+K}}\right]. \tag{10}$$

Therefore, OTL are 0 and z_{opt} on the I axis. As mentioned previously, there are three cases when false detection of the 16 QAM signal is made if the I component of the transmitted 16 QAM signal is $d/2$ (2 cases) and $3d/2$ (1 case). The error probabilities for the three cases are termed P_{IOA}, P_{IOB}, and P_{IOC}, respectively and they are specified in the following equations.

$$P_{IOA} = \int_{-\infty}^{0} p_1(z)\,dz = \frac{1}{2}\,\mathrm{erfc}\left[\sqrt{\frac{K\cdot\gamma_n\cdot\gamma_I}{5(1+K)(\gamma_n+2\gamma_I)+\gamma_n\cdot\gamma_I}}\right], \tag{11a}$$

$$P_{IOB} = \int_{-\infty}^{z_{opt}} p_2(z)\,dz = \frac{1}{2}\,\mathrm{erfc}\left[\sqrt{\frac{4(K+1)\cdot\gamma_n\cdot\gamma_I}{5(K+1)(\gamma_n+2\gamma_I)+9\gamma_n\cdot\gamma_I}}\cdot\left(\frac{3}{2}\sqrt{\frac{K}{K+1}}-B\right)\right], \tag{11b}$$

$$P_{IOC} = \int_{z}^{\infty} p_2(z)\,dz = \frac{1}{2}\,\mathrm{erfc}\left[\sqrt{\frac{4(K+1)\cdot\gamma_n\cdot\gamma_I}{5(K+1)(\gamma_n+2\gamma_I)+9\gamma_n\cdot\gamma_I}}\cdot\left(B-\frac{1}{2}\sqrt{\frac{1}{K+1}}\right)\right]. \tag{11c}$$

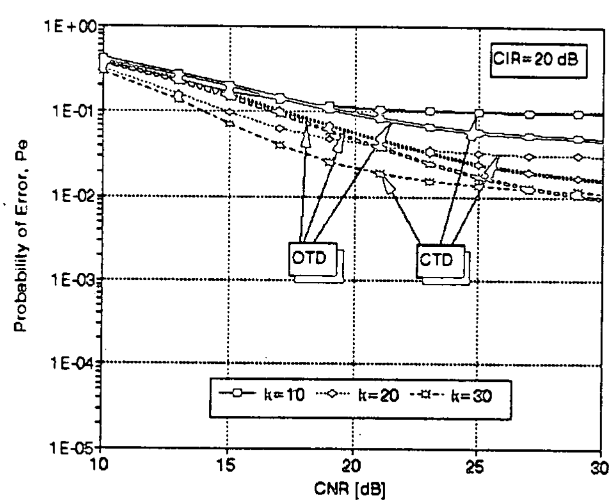

Fig. 4. The error performance of 16 QAM signal in the Rician fading channel(CIR=20 dB).

where

$$B = \frac{3}{8}\left[\frac{\sqrt{K}+\sqrt{K+\ln 3}}{\sqrt{1+K}}\right].$$

Approaching similarly for the case of CTD, it is fairly easy to show that the average error performance of 16 QAM signal with OTD in the Rician fading environment becomes

$$P_{EO} = P_{IOA} + P_{IOB} + P_{IOC}. \tag{12}$$

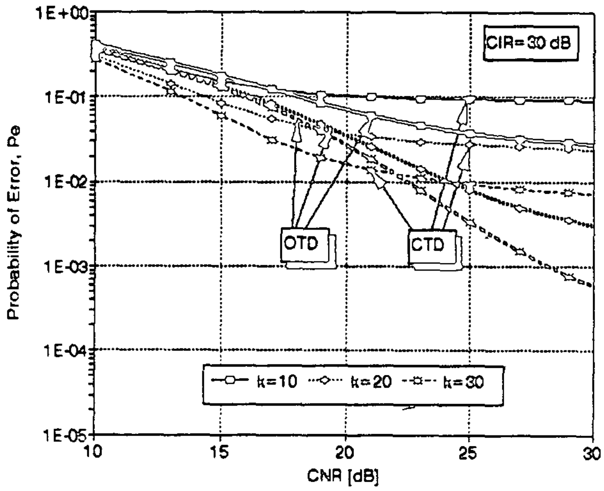

Fig. 5. The error performance of 16 QAM signal in the Rician fading channel(CIR=30 dB).

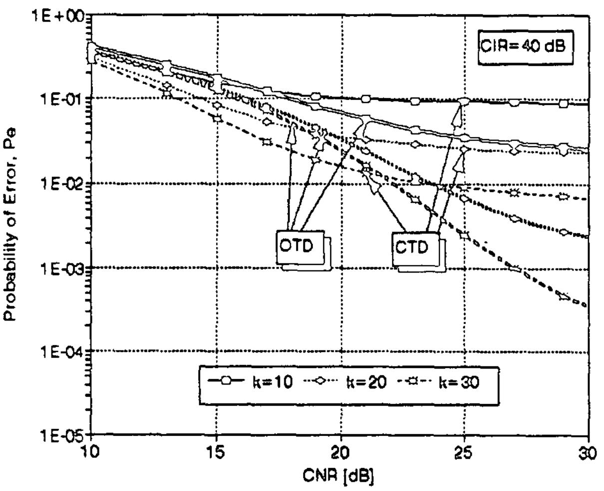

Fig. 6 The error performance of 16 QAM signal in the Rician fading channel(CIR=40 dB).

Figs. 4, 5 and 6 illustrate the error performance of the 16 QAM signal in the Rician fading channel in the presence of cochannel Rayleigh interference when CTD and OTD are selectively used in the demodulator. As shown in the figures, in the lower CIR region. ($\leq$20 dB) the effect of CIR values on the error performance is greater than that of K values which is represented as fading depth but if CIR values are more than about 30 dB, the effect of CIR values on the error performance is actually neglected and the effect of K values is dominant on the error performance. In the fig. 5 when CIR=30 dB and CNR=30 dB the error rate with CTD is 9×10^{-2} for K=10 and 7×10^{-3} for K=30. The error performance with OTD is 2.6×10^{-2} for K=10 and 3.1×10^{-4} for K=30. Thus, the performance with OTD is relatively better than that of CTD. However, to visualize the 16 QAM in a commercial system, a further improvement in its performance is necessary due to its inherent large error rate.

IV. Improvement Of Error Performance By Diversity

The envelope of the received signal, r_i, corrupted by the Rician fading is Rician distributed as follows ;

$$p(r_i)=\frac{r_i}{\psi_0}\exp\left\{-\frac{r_i^2+A^2R_0^2}{2\psi_0}\right\}I_0\left(\frac{r_iAR_0}{\psi_0}\right) \tag{13}$$

where $I_0(\ )$ is the modified Bessel function of the first kind of order zero, $(AR_0)^2/2$ is the power of the direct component, and ψ_0 is the power of the diffuse component.

By a simple change of variables in the pdf in the Eq. (13), we obtain the pdf of the instantaneous signal to interference plus noise ratio, $\gamma_i\left(=\frac{r_i^2}{2(\sigma_n^2+\sigma_I^2)}\right)$, in the form

$$p(\gamma_i)=\frac{K}{A^2\Gamma}\exp\left\{-\frac{K}{A^2\Gamma}\gamma_i-K\right\}I_0\left(2\sqrt{\frac{K^2}{A^2\Gamma}\gamma_i}\right) \tag{14}$$

where $K = A^2R_0^2/2\psi_0$ and Γ is the average signal received to interference plus noise ratio $\left(=\frac{R_0^2}{2(\sigma_n^2+\sigma_I^2)}\right)$.

Assuming that the received 16 QAM signal corrupted by the Rician fading in each diversity branch are uncorrelated, we derived the pdf of the output instantaneous signal to interference plus noise ratio, $p_M(\gamma_s)$, at the M-branch MRC diversity reception circuit which is derived in Appendix, based on the procedure given in the reference[9].

$$p_M(\gamma_s) = \frac{(1+K)\gamma_s^{\frac{M-1}{2}}}{\Gamma}\left(\frac{1+K}{KM\Gamma}\right)^{\frac{M-1}{2}}\cdot\exp\left\{-\left(\frac{MK\Gamma+(1+K)\gamma_s}{\Gamma}\right)\right\}\cdot I_{M-1}\left(2\sqrt{\frac{K(1+K)M\gamma_s}{\Gamma}}\right). \tag{15}$$

The symbol error performance of 16 QAM signal with CTD and OTD is given in the Eqs. (16a) and (16b) respectively.

$$P_{EC-MRC} = \int_0^{\infty} P_C(\gamma_s)\,p_M(\gamma_s)\,d\gamma_s, \tag{16a}$$

where $P_C(\gamma_s) = \frac{1}{2}\mathrm{erfc}\left[\sqrt{\frac{\gamma_s}{10}}\right]$

$$P_{EO-MRC} = \int_0^{\infty} P_O(\gamma_s)\, p_M(\gamma_s)\, d\gamma_s \qquad (16b)$$

where

$$P_O(\gamma_s) = \frac{1}{2}\left\{ \mathrm{erfc}\left(\sqrt{\frac{\gamma_s}{10}}\right) + \mathrm{erfc}\left[\frac{3}{4}\left(4 - \frac{\sqrt{K}+\sqrt{K+\ln 3}}{\sqrt{1+K}}\right)\sqrt{\frac{\gamma_s}{10}}\right] + \mathrm{erfc}\left[\frac{1}{4}\left(\frac{3\sqrt{K}+\sqrt{K+\ln 3}}{\sqrt{1+K}} - 4\right)\sqrt{\frac{\gamma_s}{10}}\right] \right\}.$$

In eq. (16b), $P_O(\gamma_S)$ is the error performance of OTD in AWGN and Rayleigh interference. In this case, $p_1(z)$ and $p_2(z)$ are as follows.

$$p_1(z) = \frac{1}{\sqrt{2\pi(\sigma_I^2 + \sigma_n^2)}} \exp\left\{ - \frac{(z - \frac{d}{2})^2}{2(\sigma_I^2 + \sigma_n^2)} \right\}, \qquad (17a)$$

$$p_2(z) = \frac{1}{\sqrt{2\pi(\sigma_I^2 + \sigma_n^2)}} \exp\left\{ - \frac{(z - \frac{3d}{2})^2}{2(\sigma_I^2 + \sigma_n^2)} \right\}. \qquad (17b)$$

Using eq. (17a) and eq. (17b), $P_O(\gamma_S)$ is derived as the procedure of section Ⅲ.2.

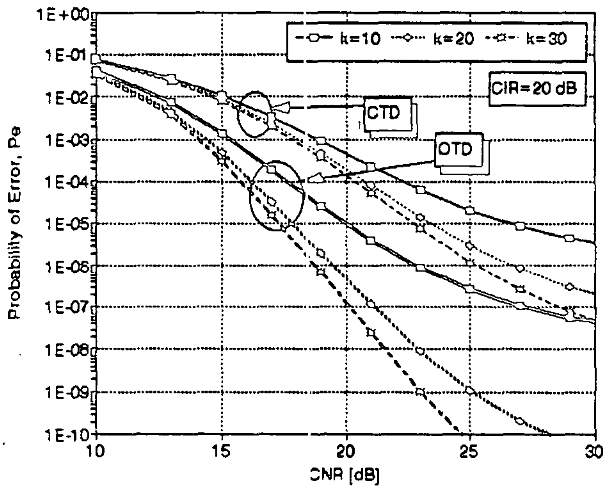

Fig. 7 The error performance of 16 QAM signal in the Rician fading channel when MRC diversity is adopted(CIR=20 dB).

The numerical evaluation of the Eqs. (16a) and (16b) are plotted in Figs. 7, 8, and 9 varying CIR values from 20 dB to 40 dB by step of 10 dB. The figures show that the error performance of the 16 QAM signal is well improved when the MRC diversity is adopted. And the performance of OTD is relatively better than that of CTD. As shown in fig. 7 (CIR=20 dB), we observed that OTD outperforms CTD by about 5.4~6.8 dB when the error rate is 10^{-5} with K varying from 30 to 10. Therefore, in the lower CIR region(CIR≤20 dB), as the fading is more serious, the OTD provides the more improvement of performance in CNR over CTD in order to achive good error performance for data communications. In Fig. 8 and 9, when the error rate is 10^{-5} and K=10, in the case of CTD, CNR is about 21.7 dB (for CIR=30 dB) and 21.3 dB(for CIR=40 dB). In the case of OTD, CNR=18.3 dB (for CIR=30 dB) and 18.1dB (for CIR=40 dB) When the error rate is 10^{-5} and K=30, in the case of CTD, CNR is about 20 dB(for CIR=30 dB) and 19.8 dB(for CIR=40 dB). In the case of OTD, CNR=16.2 dB (for CIR=30 dB) and 16.1 dB (for CIR=40 dB) Therefore, if CIR values are more than 30 dB, we can neglect the effect of CIR values on the error performance and the OTD provides the performance improvement of about 3.2~3.8 dB in CNR over CTD without regard to K when error rate is 10^{-5}.

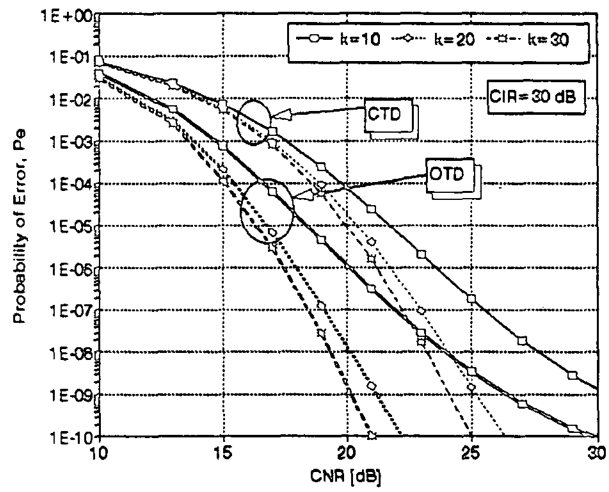

Fig. 8. The error performance of 16 QAM signal in the Rician fading channel when MRC diversity is adopted (CIR=30 dB).

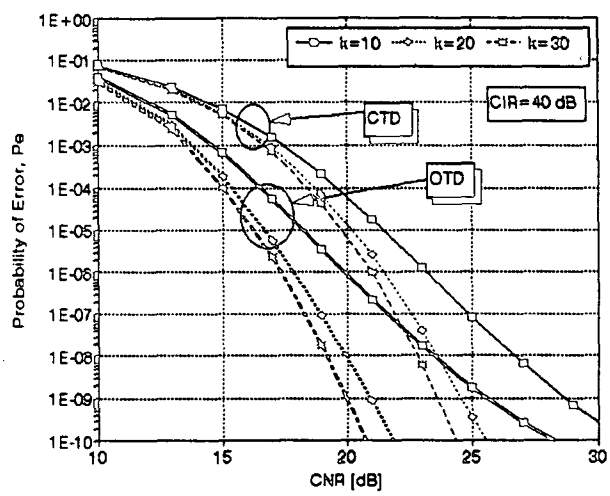

Fig. 9. The error performance of 16 QAM signal in the Rician fading channel when MRC diversity is adopted (CIR=40 dB).

V. Conclusions

With the result of analysis, we know that there exist a synergistic effect due to MRC diversity and optimum threshold detection in the Rician/Rayleigh fading channel. Having the MRC diversity reception, in the lower CIR region (CIR≤20 dB), as the fading is more serious, the OTD provides the more improvement of performance in CNR over CTD in order to achive good error performance for data communications. But if CIR values are more than about 30dB, the OTD provides the performance improvement of about 3.2~3.8dB in CNR over CTD without regard to fading depth.

Appendix

M-branches Maximal Ratio Combiner results in an instantaneous output signal to interference plus noise ratio which is the sum of the instantaneous signal to interference plus noise ratio's on the individual branches,

$$\gamma_s = \sum_{i=0}^{M} \gamma_i \qquad (A.1)$$

The characteristic function of the instantaneous signal to interference plus noise ratio, γ_i, is defined by

$$g_i(u) = \overline{\exp(ju\gamma_i)} = \int_{-\infty}^{\infty} \exp(ju\gamma_i) p(\gamma_i) d\gamma_i$$

$$= \int_0^{\infty} \exp(ju\gamma_i) \frac{K+1}{\Gamma} \exp\left(-K - \frac{\gamma_i(K+1)}{\Gamma}\right) I_0\left(2\sqrt{\frac{\gamma_i K(K+1)}{\Gamma}}\right) d\gamma \qquad (A.2)$$

Using the formula[10],

$$\int_0^{\infty} x^{v-1} \exp(-ux^p) dx = \frac{1}{|p|} u^{v/p} \Gamma\left(\frac{v}{p}\right)$$

The characteristic function, $g_i(u)$, becomes

$$g_i(u) = \frac{K+1}{K+1-ju\Gamma} \exp\left(-K + \frac{K^2+K}{K+1-ju\Gamma}\right) \qquad (A.3)$$

Therefore, characteristic function of the sum of received signal to interference plus noise ratio is

$$g(u) = \prod_{i=1}^{M} g_i(u)$$

$$= \left(\frac{K+1}{K+1-ju\Gamma}\right)^M \exp\left(-KM + \frac{(K^2+K)M}{K+1-ju\Gamma}\right) \qquad (A.4)$$

The p.d.f. of instantaneous output signal to interference plus noise ratio is obtained as

$$p_M(\gamma_s) = F[g(u)]$$

$$= \frac{1}{2\pi} \int_{-\infty}^{\infty} g(u) \exp(-ju\gamma_s) du$$

$$= \frac{1}{2\pi} \left(\frac{K+1}{\Gamma}\right)^M \exp(-KL)$$

$$\cdot \int_{-\infty}^{\infty} \left(\frac{\Gamma}{K+1-ju\Gamma}\right)^M \exp\left(-ju\gamma_s + \frac{(K^2+K)M}{K+1-ju\Gamma}\right) du \qquad (A.5)$$

Using the formula[11],

$$I_0(z) = \frac{1}{2\pi j} \int_{c-j\infty}^{c+j\infty} \frac{1}{p} \exp\left\{\frac{z}{2}\left(p + \frac{1}{p}\right)\right\} dp, \quad c>0$$

$$= \frac{1}{2\pi j} \oint_c \frac{1}{p} \exp\left\{\frac{z}{2}\left(p + \frac{1}{p}\right)\right\} dp$$

$$I_n(ab) = \frac{1}{2\pi j} \left(\frac{b}{a}\right)^n \oint_c \frac{1}{s^{n+1}} \exp\left(\frac{a^2}{2} s + \frac{b^2}{2} \frac{1}{s}\right) ds$$

The p.d.f. of instantaneous output signal to interference plus noise ratio is derived as

$$p_M(\gamma_s) = \frac{(1+K)\gamma_s^{\frac{M-1}{2}}}{\Gamma} \left(\frac{1+K}{KM\Gamma}\right)^{\frac{M-1}{2}} \cdot \exp\left\{-\left(\frac{MK\Gamma + (1+K)\gamma_s}{\Gamma}\right)\right\}$$

$$\cdot I_{M-1}\left(2\sqrt{\frac{K(1+K)M\gamma_s}{\Gamma}}\right). \qquad (15)$$

References

[1] D. J. Goodman, "Trends in cellular and cordless communications," IEEE Commun., Mag., pp. 31-40, June 1991.

[2] I. M. Ross and AT&T Bell Lab., "Wireless network directions," IEEE Commun., Mag., vol. 29, no. 2, pp. 40-42, Feb. 1991.

[3] R. J. C. Bultitude, and G.K. Bedal, "Propagation characteristics on microcellular urban mobile radio channel at 910 MHz, " IEEE J. on Selected Areas in Communication, vol. SAC-7, no. 1, pp. 31-39, Jan. 1989.

[4] Y. D. Yao and A. U. H. Sheikh, "Outage probability analysis for microcell mobile radio systems with cochannel interferers in Rician/ Rayleigh fading environments," Electro. Lett., vol. 26. pp. 864-866, June 1990.

[5] N. Morinaga, S. Komaki and S. Hara, "Trends in modulation/demodulation and coding techniques for mobile satellite communications systems," IEICE (Japan) Trans. Commun., vol. E74, no. 8, pp. 2211-2219, Aug. 1991.

[6] E. G. Kim, B. J. Ko and S. J. Cho, "Optimum threshold detection of 16 QAM signal in Rician fading channel," Asia-Pacific Conf. on Com. (APCC'93), Taejon, Korea, vol. 2, pp. 462-467, Aug. 1993.

[7] J. G. Proakis, *Digital Communications.* 2nd ed., New York: McGraw-Hill, 1989.

[8] R. D. Gitlin, J. F. Hayes, and S. B. Weinstine, *Data*

Communications Principles. New York: Plenum Press, 1992.

[9] M. Schwartz, *Communication Systems and Techniques.* New York: McGraw-Hill, 1966.

[10] I. S. Gradshteyn and I M. Ryzhik, *Tables of Integrals of Series and Products.* New York: Academic Press, 1980.

[11] Mischa Schwartz, Willaim R. Bennett and Seymour Stein, *Communication Systems and Techniques.* McGraw-Hill, 1966.

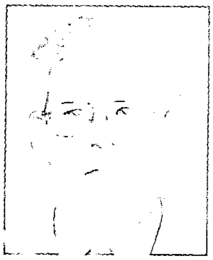

Eon Gon Kim was born in Busan, Korea, on March 8, 1958. He received a B.E. degree in Communication Engineering and a M.E. degree in Avionics Engineering from Hankuk Aviation University, Kyunggi-Do, Korea, in 1982 and 1985, respectively. From 1984 to 1995 he was involved in developing a cellular phone in Wireless Comm, Group Telecomm. R & D Center, Samsung Electronics. He is currently working towards a Ph.D. degree in Avionics Engineering at Hankuk Aviation University. Since 1995, he has been a full-time lecturer in the Department of Information and Telecommunication Engineering at Taejeon national University of Technology. His current interest fields are mobile and stellite communications.

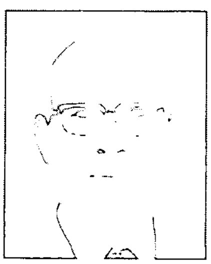

Sung Joon Cho was born in Seoul, Korea, on January 9, 1946. He received a B.E. degree, with Highest Distinction, in Communication Engineering from Hankuk Aviation University, Kyunggi-Do, Korea, in 1969, a M.E. degree in Communication Engineering from Hanyang University, Seoul Korea, in 1975, and a Ph.D. degree in Communication Engineering from Osaka University, Osaka Japan, in 1981. From 1969 to 1972, he served as a Korean Naval Officer. Since August 1972, he has been with the Department of Telecommunication and Information Engineering at Hankuk Aviation University and currently is a Professor there. He studied abroad in Japan. His past appointments at Hankuk Aviation University include : Dean of Student Affairs Division and Dean of Academic Affairs Division. He is a member of the Board of Directors of Korea Electromagnetic Engineers Society (KEES) and a member of the Board of Directors of Korean Institute of Communication Sciences (KICS). He was the Editor-in-Chief of Transaction at KICS. Also, he is a member of IEEE, Institute of Electronics, Information and Communication Engineers of Japan (EIC) and Institute of Television Engineers of Japan (ITE). He received a prize for scientific research from KICS in 1984, from KEES in 1994 and from Hankuk Aviation University in 1995. His research interests are in the fields of communication systems, mobile radio communications and satellite communications.

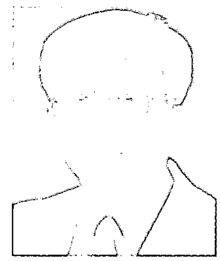

Chang Heon Oh was born in Seoul, Korea, on February 10, 1965. He received B.E. and M.E. degrees in Telecommunication and Information Engineering from Hankuk Aviation University, Kyunggi-Do, Korea, in 1988 and 1990, respectively. He will be receiving his Ph.D. degree in February 1996 from Hankuk Aviation University. In 1990, he joined Hanjin Electronics Co., where he was involved in the research and development of radio communication monitoring systems. Since 1993, he has been in the Communication Systems R & D Center of Samsung Electronics Co. He is currently involved in the research and development of the CDMA cellular system.